

Robust Trajectory Planning for a Multirotor Using Funnel Library

Suseong Kim¹, Davide Falanga¹ and Davide Scaramuzza¹

Abstract—This paper is about funnel library that can be used to generate robust trajectories for multirotors.

I. INTRODUCTION

Throughout the paper, 0_{ij} stands for the zero matrix in $\mathbb{R}^{i \times j}$, and I_i denotes the identity matrix in $\mathbb{R}^{i \times i}$. For a matrix, $\|\cdot\|$ represents the induced 2 norm, and $\lambda_{\max}(\cdot)$ and $\lambda_{\min}(\cdot)$ indicate the maximum and minimum eigenvalues. Also, $|\cdot|$ is the Euclidean norm for a vector. For two vectors $\alpha, \beta \in \mathbb{R}^{3 \times 1}$, we denote the inner and cross products as $\langle \alpha, \beta \rangle = \alpha^\top \beta$ and $\mathbf{S}(\alpha)\beta = \alpha \times \beta$. For two quaternions \mathbf{q}_1 and \mathbf{q}_2 , the quaternion multiplication expressed as $\mathbf{q}_1 \otimes \mathbf{q}_2$. Also, $\mathbf{P}(\cdot)$ is the quaternion representation of a vector $\omega \in \text{so}(3)$ such as $\mathbf{P} = [0 \ \omega^\top]^\top$. The rotation of a vector is indicated as $\mathbf{q}_1 \odot \omega = \mathbf{q}_1 \otimes \mathbf{P}(\omega) \otimes \mathbf{q}_1^{-1}$. Furthermore, $\text{c} \cdot$ and $\text{s} \cdot$ are shorthands of $\cos \cdot$ and $\sin \cdot$, respectively.

II. QUADROTOR DYNAMICS AND CONTROL

A. Quadrotor dynamics

To describe the dynamic model of a multirotor, we define the inertial $O_I\{x_I, y_I, z_I\}$ and the multirotor body-fixed $O_b\{x_b, y_b, z_b\}$ frames. The body-fixed frame is located at the center of the multirotor. The translational and angular dynamics of a multirotor is described as follows:

$$\ddot{p} = gz_I + Tz_b + F_d + \delta \quad (1)$$

$$\dot{\mathbf{q}} = \frac{1}{2}\mathbf{q} \otimes \mathbf{P}(\omega) \quad (2)$$

where p is the position of O_b with respect to O_I , and $\mathbf{q} = [q_0 \ \bar{\mathbf{q}}^\top]^\top$ is the unit quaternion describing the orientation of O_b with respect to O_I . The angular velocity of O_b represented in O_b is denoted as ω . The terms g and T are gravitational constant and mass normalized collective thrust, respectively. Without loss of generality, the axis z_I is defined as $e_3 = [0 \ 0 \ 1]^\top$. The rotor drag applied on the multirotor is denoted as F_d , and it is explicitly expressed as follows:

$$F_d = c_d \mathbf{q} \odot \pi_z \mathbf{q}^{-1} \odot \dot{p} \quad (3)$$

where c_d is the rotor drag coefficient, $\pi_z = I_3 - e_3 e_3^\top$ is the matrix projecting a vector onto the $x_b y_b$ plane. The external forces and model uncertainties excluding the rotor drag term are lumped in $\delta \in \mathbb{R}^{3 \times 1}$.

In eq. (2), angular velocity ω is used as the input term since the rotational velocity dynamics is fast enough. It is possible based on the assumption that the multirotor body angular rate ω could be directly controlled with low-level controllers such

as [DANDREA] or off-the-shelf flight controllers supporting angular rate control mode. Therefore, the input terms of the multirotor dynamics in eqs. (1) and (2) are T and ω .

Uncertainty and disturbances In the free flight scenario, rotor drag and fuselage drag could be considered as the biggest external disturbances. The rotor drag could be modeled as, and the fuselage drag could be blah blah. Non perfect input tracking, XXX

B. Multirotor control

Let us assume that the reference trajectory of the differential flat output[MEL], which are $\{p(t)^r, \psi^r(t)\}$ and \mathcal{C}^2 , are given. Here, $p^r(t)$ is the reference trajectory of the multirotor, and $\psi(t)$ represents the reference rotation of the multirotor about the z_b body axis, i.e. yaw angle in the Euler attitude representation.

To control the translational motion of a multirotor, we utilized a geometric control method [TYL] which is widely utilized in the researches on multirotors [RPG][UPENN][MIT]. Let $e_p = p - p^r$ and $e_v = \dot{p} - \dot{p}^r$ be the position and velocity error terms. With the above definitions, the mass normalized thrust T and desired thrust direction of a multirotor z_b^d could be computed as the following procedure:

$$\begin{aligned} \ddot{p}^d &= -K_p e_p - K_v e_v - g e_3 + \ddot{p}^r \\ z_b^d &= \ddot{p}^d / |\ddot{p}^d| \\ T &= \langle \ddot{p}^d, z_b \rangle = |\ddot{p}^d| \langle z_b^d, z_b \rangle \end{aligned} \quad (4)$$

where K_p and K_v are gain matrices with positive diagonal entries. By substituting the terms T and \ddot{p}^d in (1), the error dynamics of the translational motion could be derived as follows:

$$\begin{aligned} \ddot{e}_p &= g e_3 + T z_b + F_d + \delta - \ddot{p}^r + \ddot{p}^d - \ddot{p}^d \\ &= -K_p e_p - K_v e_v + F_d + \delta + T z_b - \ddot{p}^d \\ &= -K_p e_p - K_v e_v + F_d + \delta + |\ddot{p}^d| \{ \langle z_b^d, z_b \rangle z_b - z_b^d \} \\ &= -K_p e_p - K_v e_v + F_d + \delta + |\ddot{p}^d| s_\Phi u \end{aligned} \quad (5)$$

where Φ is the angle between the axes z_b and z_b^d , and u is the unit vector indicating the direction of the term inside of the curly bracket.

Similarly, the rotational motion of a multirotor could be analyzed by combining it with a control law that generates the desired angular rate ω^d . First, we compute the desired attitude of the multirotor with $\psi(t)$ and z_b^d as follows: [MEL]

$$\begin{aligned} \bar{y}_b &= [-s_{\psi^r} \quad c_{\psi^r} \quad 0]^\top \\ x_b^d &= \mathbf{S}(\bar{y}_b) z_b^d / |\mathbf{S}(\bar{y}_b) z_b^d| \\ y_b^d &= \mathbf{S}(z_b^d) x_b^d / |\mathbf{S}(z_b^d) x_b^d|. \end{aligned}$$

*This work was not supported by any organization

¹S. Kim is with the Robotics and Perception Group, University of Zurich, Switzerland {suseong, falanga, sdavide} at ifi.uzh.ch

Then, based on the axes $\{x_b^d, y_b^d, z_b^d\}$, the desired coordinate could be represented with the unit quaternion \mathbf{q}^d . The attitude error between \mathbf{q}^d and \mathbf{q} is denoted as $\mathbf{q}_e = \mathbf{q}^{-1} \otimes \mathbf{q}^d$. To decrease the attitude error $\mathbf{q}_e = [q_e \ \bar{q}_e^\top]^\top$, the angular velocity is set as

$$\omega = \begin{cases} \omega_d^d - k_p \bar{q}_e & \text{if } q_e \geq 0, \\ \omega_d^d + k_p \bar{q}_e & \text{if } q_e < 0. \end{cases} \quad (6)$$

where ω_d^d is the desired angular velocity of \mathbf{q}^d represented in \mathbf{q}^d . According to [ETH], the attitude error \mathbf{q}_e is globally asymptotically stable equilibrium point. Hence, it is possible to assume that the error Φ is also asymptotically stable, and bounded by a known value.

Assumption : In this work, we assume that the norm of the external disturbance is bounded as $|\delta| \leq \bar{\delta}$. Also, the norm of the nominal mass normalized collective thrust value is bounded as $|ge_3 + \ddot{p}^r| \leq \bar{T}$ given any \mathcal{C}^2 reference trajectory x^r . Furthermore, the maximum thrust axis error is bounded such as $s_\Phi \leq \bar{s}_\Phi$.

C. Stability analysis

In Sec. II-B, it is assumed that the attitude error is bounded for all flight duration. In this subsection, we investigate the stability of the translational dynamics in eq. (5). As the first step, the dynamics system is summarized as follows:

$$\begin{aligned} \dot{e}_p &= e_v \\ \dot{e}_v &= -K_p e_p - K_v e_v + F_d + \delta + s_\Phi |\ddot{p}^d| u. \end{aligned} \quad (7)$$

To analyze the stability of the error dynamics conveniently, we assume that $K_p = k_p I_3$ and $K_v = k_v I_3$ with positive scalar gain values k_p and k_v . Then, we define the Lyapunov candidate function as $V = \frac{1}{2} e^\top P e$ where $e = [e_p^\top \ e_v^\top]^\top$ and

$$P = \begin{bmatrix} (k_p + k_d)I_3 & I_3 \\ I_3 & I_3 \end{bmatrix}.$$

The Lyapunov function is positive definite when $k_p + k_v > 1$. Furthermore, the directional derivative of V can be summarized as follows:

$$\begin{aligned} \dot{V} &= -k_p e_p^\top e_p - k_v e_v^\top e_v + e_v^\top e_v \\ &\quad + (e_p + e_v)^\top \{\delta + F_d + |\ddot{p}^d| s_\Phi u\}. \end{aligned} \quad (8)$$

Then, by having \ddot{p}^d in eq. (4), $|\delta| \leq \bar{\delta}$, $|F_d| \leq c_d |\dot{p}^r + e_v|$, and $|s_\Phi u| < \bar{s}_\Phi$, we can rearrange the above relation further as

$$\begin{aligned} \dot{V} &\leq -k_p |e_p|^2 - (k_v + 1) |e_v|^2 + (|e_p| + |e_v|) \\ &\quad \times \{\bar{\delta} + c_d |\dot{p}^r + e_v| + \bar{s}_\Phi (| -k_p e_p - k_v e_v | + \bar{T})\} \\ &\leq -\bar{e}^\top Q \bar{e} + \Delta |\bar{e}| \end{aligned} \quad (9)$$

where $\bar{e} = [|e_p| \ |e_v|]^\top$, $\Delta = \bar{\delta} + c_d |\dot{p}^r| + \bar{s}_\Phi \bar{T}$ and

$$Q = \begin{bmatrix} k_p(1 - \bar{s}_\Phi) & -\frac{1}{2}\{c_d + \bar{s}_\Phi(k_p + k_d)\} \\ -\frac{1}{2}\{c_d + \bar{s}_\Phi(k_p + k_d)\} & k_v(1 - \bar{s}_\Phi) - 1 - c_d \end{bmatrix}.$$

Here, the matrix Q can be considered as the summation of the two separated parts such as

$$Q = Q_A + \bar{s}_\Phi Q_B$$

where

$$\begin{aligned} Q_A &= \begin{bmatrix} k_p & -\frac{1}{2}c_d \\ -\frac{1}{2}c_d & k_v - 1 - c_d \end{bmatrix} \\ Q_B &= \begin{bmatrix} -k_p & -\frac{1}{2}(k_p + k_v) \\ -\frac{1}{2}(k_p + k_v) & -k_v \end{bmatrix}. \end{aligned} \quad (10)$$

By setting $k_v > 1 + c_d$ and $k_p > \frac{c_d^2}{4(k_v - 1 - c_d)}$, we can make the matrix Q_A positive definite. On the other hand, the matrix Q_B cannot be positive definite since the determinant of Q_B is $\det(Q_B) = -\frac{1}{4}(k_p - k_v)^2 \leq 0$, i.e. $\lambda_{\max}(Q_B) \geq 0$ and $\lambda_{\min}(Q_B) \leq 0$. However, even though Q_B is not positive definite, we can assure that the matrix Q is positive definite with the condition $\bar{s}_\Phi < -\lambda_{\min}(Q_A)/\lambda_{\min}(Q_B)$ which could readily be achieved since $\bar{s}_\Phi \approx 0$ with a well designed attitude controller. Therefore, with the gain values k_p and k_v fulfilling $\lambda(Q) \geq 0$, eq. (9) becomes

$$\begin{aligned} \dot{V} &\leq -\lambda_{\min}(Q) |\bar{e}|^2 + \Delta |\bar{e}| \\ &\leq -\lambda_{\min}(Q)(1 - \theta) |\bar{e}|^2 - \lambda_{\min}(Q) \theta |\bar{e}|^2 + \Delta |\bar{e}| \end{aligned}$$

where $0 < \theta < 1$. Therefore, the error dynamics of the translational system of a multirotor is uniformly ultimately bounded. Furthermore, the ultimate bound b could be computed as

$$b = \sqrt{\frac{\lambda_{\max}(P)}{\lambda_{\min}(P)}} \mu^2, \quad \mu = \frac{\Delta}{\lambda_{\min}(Q) \theta}.$$

In this analysis, we could know that any error will eventually enter into the ultimate bound $|e| \leq b$ within finite time. The ultimate bound is the function of Δ and it is the combination of $\bar{\delta}$, $|\dot{p}^r|$, and $\bar{s}_\Phi \bar{T}$. Also, the drag coefficient and the maximum attitude error could be interpreted as the weight terms. Hence, the radius of the bound will get bigger by having larger disturbances, reference velocity, and reference acceleration ($\bar{T} = |ge_3 + \ddot{p}^r|$). However, even though we could get the general sense on how the error will behave, it is difficult to know the tight ultimate bound that the error states actually resides. Also, given initial set of error states, it is hard to see how the error evolve before getting into the ultimate bound.

III. COMPUTING FUNNELS

In Sec. ??, we checked the general behaviour of the translational error dynamic system in conservative manner. However, with the funnel analysis with sum of squares optimization tools, we can find the realistic outermost bound on the state e . The concept of funnel and numerical method for computing funnel are mainly adopted from [MAJ].

A. Funnel?

Funnel $\mathcal{F}(t) \subset \mathbb{R}^{6 \times 1}$ represents the reachable set of error $e(t) \in \mathbb{R}^{6 \times 1}$ given the initial set of error $e(t_0) \in \xi_0$ and a closed-loop dynamic equation. In other words, the error $e(t_0)$ contained in the set ξ_0 will evolve only inside of the set $\mathcal{F}(t)$ for all time. These property of the funnel could be written as follows:

$$e(t_0) \in \xi_0, \ \xi_0 \subset \mathcal{F}(0) \Rightarrow e(t) \in \mathcal{F}(t), \ \forall t \geq t_0. \quad (11)$$

Define a time varying positive definite matrix $P_{\mathcal{F}}(t) \in \mathbb{R}^{6 \times 6}$, a positive parameter $\alpha(t) \in \mathbb{R}$, and $V_{\mathcal{F}}(t, e) = e(t)^\top P_{\mathcal{F}}(t) e(t)$. In the following analysis, $V_{\mathcal{F}}(t, e)$ will be a Lyapunov function, and $\alpha(t)$ will be the parameter indicating the level of $V_{\mathcal{F}}(t, e)$. Then, define a set $\mathcal{F}(t)$ as

$$\mathcal{F}(t) = \{e(t) \in \mathbb{R}^{6 \times 1} | V_{\mathcal{F}}(t, e) \leq \alpha(t)\} \quad (12)$$

with $V_{\mathcal{F}}$ and α constrained such that

$$\begin{aligned} \dot{V}_{\mathcal{F}}(t, \hat{e}) &< \dot{\alpha}(t), \\ \text{for } \hat{e}(t) &= \{e(t) | V_{\mathcal{F}}(t, e) = \alpha(t), t \in [t_0, t_f]\}. \end{aligned} \quad (13)$$

From the constraint, it is obvious that the state $e(t) \in \mathcal{F}(t)$ cannot escape the sublevel set described by $V_{\mathcal{F}}(t, e) \leq \alpha(t)$. Therefore, the set $\mathcal{F}(t)$ defined in eqs. (12) and (13) complies with the definition of funnel in eq. (11) [MAJ].

Another constraint to fulfill the property of funnel defined in eq. (11) is related on the initial condition of a funnel. At $t = t_0$, the initial set of e , i.e. ξ_0 , should be the subset of $\mathcal{F}(t_0)$. To satisfy the constraint, we define $\xi_0 = \{e \in \mathbb{R}^{6 \times 1} | e^\top R e \leq 1\}$ with a positive definite matrix R . Then, the constraint can be written as follows:

$$V_{\mathcal{F}}(t_0, \hat{e}) \leq \alpha(t_0), \text{ for } \hat{e} = \{e | e^\top R e \leq 1\}. \quad (14)$$

Furthermore, we want to find $V_{\mathcal{F}}$ and α that represent the tight outer bound of e . Since $P_{\mathcal{F}}$ is a positive definite matrix and $V_{\mathcal{F}}$ is a quadratic function of e , it is possible to define an ellipsoid that enclosing the level set defined as $V_{\mathcal{F}}(t, e) = \alpha(t)$. Then, by minimizing the size of the outer shell, the size of the funnel could be minimized consequently. The outer ellipsoid can be formulated such as

$$\begin{aligned} \hat{e}^\top(t) S(t) \hat{e}(t) &\leq 1, \\ \text{for } \hat{e}(t) &= \{e(t) | V_{\mathcal{F}}(t, e) = \alpha(t), t \in [t_0, t_f]\}. \end{aligned}$$

where $S(t) \in \mathbb{R}^{6 \times 6}$ is the positive definite matrix representing the shape of the outer shell. Note that the volume of the ellipsoid is proportional to the determinant of $S(t)$.

Based on these observations, we can formulate the optimization problem to find the tight funnel surrounding the states $e(t)$ as follows:

$$\begin{aligned} \inf_{P_{\mathcal{F}}, \alpha, S} \quad & \int_{t_0}^{t_f} \det S(t) dt \\ \text{s.t.} \quad & \dot{V}_{\mathcal{F}}(t, \hat{e}) < \dot{\alpha}(t) \text{ for } \hat{e} = \{e(t) | V_{\mathcal{F}}(t, e) = \alpha(t)\}, \\ & \hat{e}^\top S(t) \hat{e} \leq 1 \text{ for } \hat{e} = \{e(t) | V_{\mathcal{F}}(t, e) = \alpha(t)\}, \\ & V_{\mathcal{F}}(t_0, \hat{e}) \leq \alpha(t_0) \text{ for } \hat{e} = \{e | e^\top R e \leq 1\}. \end{aligned}$$

B. Computing funnel

We compute the funnels for the multirotor translational error dynamic system. First of all, we define the Lyapunov function in the quadratic form such as $V_{\mathcal{F}} = e(t)^\top P_{\mathcal{F}} e(t)$ with the time varying positive definite matrix

$$P_{\mathcal{F}}(t) = \begin{bmatrix} P_p(t) & P_{pv}(t) \\ P_{pv}(t) & P_v(t) \end{bmatrix}$$

where $P_p(t)$, $P_{pv}(t)$, and $P_v(t)$ are diagonal matrices with positive entries. Then, with eq. (7), the directional derivative

of the Lyapunov function $V_{\mathcal{F}}$ is rearranged as follows:

$$\begin{aligned} \dot{V}_{\mathcal{F}} &= -e^\top (A^\top P_{\mathcal{F}} + P_{\mathcal{F}} A) e + e^\top \dot{P}_{\mathcal{F}} e \\ &\quad + 2e^\top P_{\mathcal{F}} B (\delta + s_\Phi |\ddot{p}^d| u + F_d) \end{aligned}$$

where

$$A = \begin{bmatrix} 0_{33} & I_3 \\ -K_p & -K_d \end{bmatrix}, \quad B = \begin{bmatrix} 0_{33} \\ I_3 \end{bmatrix}.$$

In the right hand side of the above equation, the third term further developed as

$$\begin{aligned} e^\top P_{\mathcal{F}} B (\delta + s_\Phi |\ddot{p}^d| u + F_d) &\leq |e^\top P_{\mathcal{F}} B| \{\bar{\delta} + \bar{s}_\Phi (k_p |e_p| + k_v |e_v| + \bar{T}) + c_d |\ddot{p}^r| + e_v|\} \\ &\leq (p_{pv} |e_p| + p_v |e_v|) \{\bar{s}_\Phi (k_p |e_p| + k_v |e_v|) + c_d |e_v| + \Delta\} \end{aligned} \quad (15)$$

where p_{pv} , p_v , k_p , and k_v are maximum eigenvalues of P_{pv} , P_v , K_p , and K_v . Also, $\Delta = \bar{\delta} + c_d |\ddot{p}^r| + \bar{s}_\Phi \bar{T}$. To handle the error states with the norm $|e_p|$ and $|e_v|$ in eq. (15), we define two variables $\bar{e}_p \in \mathbb{R}$ and $\bar{e}_v \in \mathbb{R}$ with the following constraints:

$$\begin{aligned} \bar{e}_p^2 &= e_p^\top e_p = |e_p|^2, \quad \bar{e}_p \geq 0 \\ \bar{e}_v^2 &= e_v^\top e_v = |e_v|^2, \quad \bar{e}_v \geq 0. \end{aligned}$$

Then, $\dot{V}_{\mathcal{F}}$ is further developed as follows:

$$\begin{aligned} \dot{V}_{\mathcal{F}} &\leq -e^\top (P_{\mathcal{F}} A + A^\top P_{\mathcal{F}}) e + e^\top \dot{P}_{\mathcal{F}} e \\ &\quad + 2(p_{pv} \bar{e}_p + p_v \bar{e}_v) \{\bar{s}_\Phi (k_p \bar{e}_p + k_v \bar{e}_v) + c_d \bar{e}_v + \Delta\}. \end{aligned} \quad (16)$$

In terms $V_{\mathcal{F}}$ and $\dot{V}_{\mathcal{F}}$, the variables of the optimization problem are continuous in t . However, to make the optimization problem easier to solve, we discretized the variables $P_{\mathcal{F}}$, α , and S . Then, the optimization problem can be reformulated as the following:

$$\begin{aligned} \inf_{P_{\mathcal{F}}(n), \alpha(n), S(n), p_{pv}(n), p_v(n)} \quad & \sum_{n=0}^N \det(S(n)) \\ \text{s.t.} \quad & \dot{\alpha}(n) - \dot{V}_{\mathcal{F}}(n) \geq 0 \text{ with constraints } c_1 \text{ to } c_9, \\ & 1 - e^\top S(n) e \geq 0 \text{ with constraints } c_9 \text{ and } c_{10}, \\ & \alpha(0) - V_{\mathcal{F}}(0) \geq 0 \text{ with constraint } c_{11}. \end{aligned} \quad (17)$$

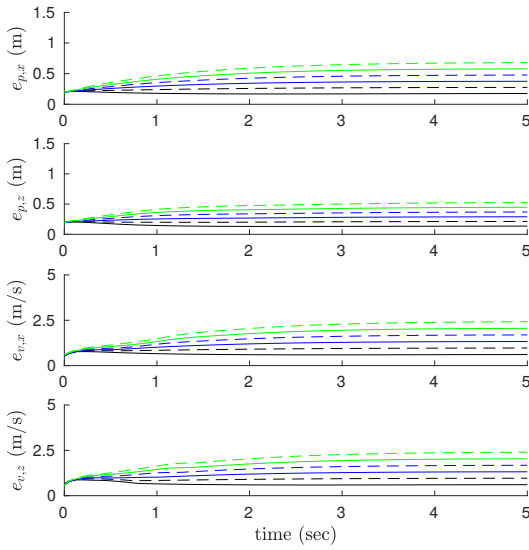
where

$$\begin{aligned} c_1 : \quad & \bar{e}_p^2 = e_p^\top e_p, & c_2 : \quad & \bar{e}_p \geq 0 \\ c_3 : \quad & \bar{e}_v^2 = e_v^\top e_v, & c_4 : \quad & \bar{e}_v \geq 0 \\ c_5 : \quad & p_{pv}(n) I_3 \geq P_{pv}(n), & c_6 : \quad & p_{pv}(n) I_3 \geq -P_{pv}(n) \\ c_7 : \quad & p_v(n) I_3 \geq P_v(n), & c_8 : \quad & p_v(n) I_3 \geq -P_v(n) \\ c_9 : \quad & \alpha(n) - V_{\mathcal{F}}(n) = 0, & c_{10} : \quad & S(n) > 0 \\ c_{11} : \quad & 1 - e^\top R e = 0. \end{aligned}$$

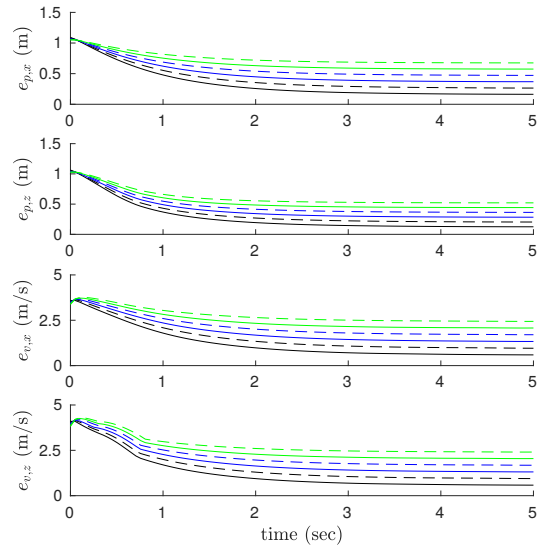
The constraints c_5 to c_8 is added to ensure $p_{pv}(n) \geq \|P_{pv}(n)\|$ and $p_v(n) \geq \|P_v(n)\|$ with diagonal matrices $P_{pv}(n)$ and $P_v(n)$. In addition, $P_{\mathcal{F}}(n)$ and $\dot{\alpha}(n)$ could be implemented as

$$\dot{P}_{\mathcal{F}}(n) = \frac{P_{\mathcal{F}}(n+1) - P_{\mathcal{F}}(n)}{dt}, \quad \dot{\alpha}(n) = \frac{\alpha(n+1) - \alpha(n)}{dt}.$$

The optimization problem in eq. (17) could be transformed into the form of sum-of-squares problem and solved efficiently by referring [MAJ].



(a) funnels computed with the initial region with r_2 .



(b) funnels computed with the initial region with r_1 .

Fig. 1: funnels computed with various values of δ . the detailed parameters and settings are available in table. I.

C. Funnel library

In the optimization problem, the list of parameters are : the initial set of error states ξ_0 ; the gain matrices K_p and K_d ; the norm of maximum attitude angle error \bar{s}_Φ ; the rotor drag coefficient c_d ; and the lumped disturbance term Δ . Among these parameters, the gain matrices are set by operator to satisfy the required flight performance in accordance with applications. The attitude error \bar{s}_Φ and drag coefficient c_d terms should be selected to be comparable with respect to the actual values. Accordingly, the terms K_p , K_d , c_d , and \bar{s}_Φ can be set with the current setting of the multirotor. However, the lumped disturbance term $\Delta(= \bar{\delta} + c_d|\dot{p}^r| + \bar{s}_\Phi|ge_3 + \ddot{p}^r|)$ keeps changing while a multirotor is in flight. For example, the external disturbance, e.g. wind condition, could be different location to location. Also, the reference velocity \dot{p}^r and accelerations \ddot{p}^r are the function of the reference trajectory so that the terms $|\dot{p}^r|$ and $|ge_3 + \ddot{p}^r|$ will change while the multirotor in maneuver. According to the stability analysis in Sec. ??, the radius of the ultimate bound varies with different Δ , and the behavior of the error states will also be altered with respect to Δ . Therefore, we evaluate funnel with various values of Δ , and use them depending on the flight condition. For example, if the external force information is available apriori δ , the rest terms \dot{p}^r and \ddot{p}^r are directly computable with the reference trajectory. Therefore, before flight operation, we can guess Δ and look up the library of funnel to see the region that error states can reside while in flight.

For example, we have generated funnels with the setting in table I. Funnels are optimized with the Δ s for every 0.1 from 0.3 to 2.5 [$m s^{-2}$]. The computed funnels are displayed in fig. 1.

Analysis on the funnels in fig. 1 by comparing the theoretical stability characteristic and the computed funnels.

param	value	param	value
dt	0.05 [s]	N	200
$K_{p,x}$	10 [s^{-2}]	$K_{v,x}$	4 [s^{-1}]
$K_{p,y}$	10 [s^{-2}]	$K_{v,y}$	4 [s^{-1}]
$K_{p,z}$	15 [s^{-2}]	$K_{v,z}$	6 [s^{-1}]
\bar{s}_Φ	0.035 [.] $\approx \sin 2^\circ$	R_1	diag([1.0 1.0 1.0 0.1 0.1 0.1]) [$m^{-2}, m^{-2}s^2$]
c_d	0.31 [s^{-1}]	R_2	diag([39 39 39 1.6 1.6 1.6])

TABLE I: parameters used for computing funnel library

D. Combining funnels

Pseudo-code for combining funnels will be presented and explained.

E. Funnel for robust trajectory generation

Once we have a multirotor and a reference trajectory, we can compute funnel around the reference trajectory. To check whether the given trajectory robust or not with respect to the obstacles, we can do collision check with the funnel and obstacles.

The method for checking collision between funnel and obstacles will be explained in detail.

IV. SIMULATIONS

Monte Carlo simulation will be inserted to show that the funnel can encapsulate the error trajectories as supposed.

A. Simulation setup

Simulation setup will be explained. Environment would be the Gazobo integrated with RotorS UAV simulator which explicitly incorporating the rotor drag terms. Multirotor will follow the minimum snap trajectories generated with to connect randomly generated waypoints. The initial condition is also randomly generated inside of the ultimate bound. Hence, the goal of the simulation is to show that the

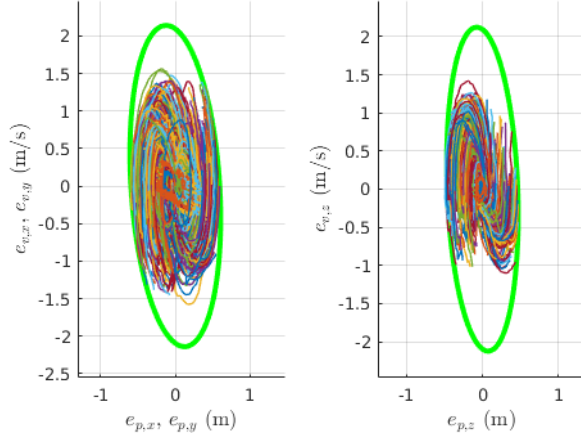


Fig. 2: The green ellipse is the ultimate bound projected to each coordinate. Since the gains $K_{p,x}$ and $K_{p,y}$, and $K_{v,x}$ and $K_{v,y}$ are set to same values, errors on x and y coordinates are displayed in the same figure.

trajectories starting inside of the ultimate bound (evaluated with the computed funnel) cannot escape the ultimate bound.

B. Simulation results

Plan is to giving explanation with the following style figure 2

V. EXPERIMENTS

Experimental scenario is the following. We want to find the *safe* velocity that a multirotor can go through a pipe type object as shown in fig. 3.

A. Experimental setup

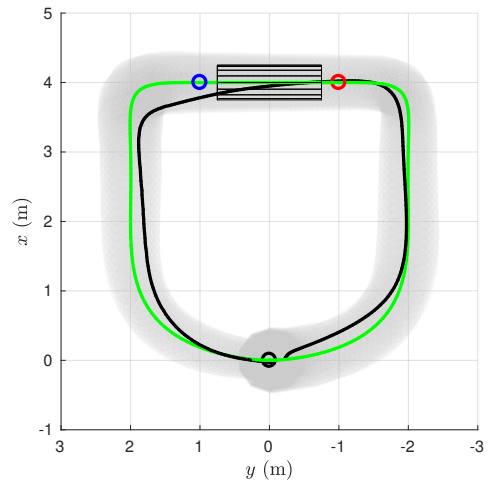
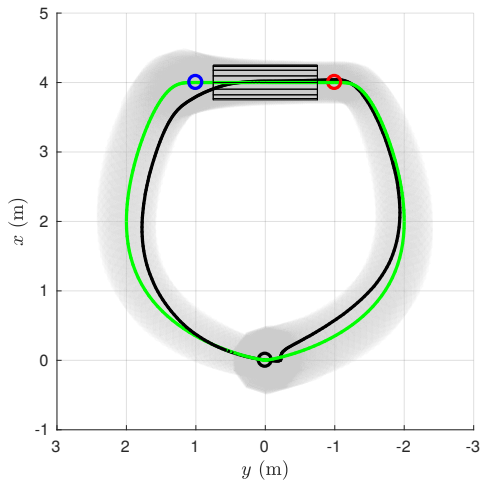
B. Experimental results

VI. CONCLUSIONS

ACKNOWLEDGMENT

REFERENCES

- [1] G. O. Young, Synthetic structure of industrial plastics (Book style with paper title and editor), in *Plastics*, 2nd ed. vol. 3, J. Peters, Ed. New York: McGraw-Hill, 1964, pp. 1564.



(a) The reference speed between the blue and red points is 1.0 m/s. (b) The reference speed between the blue and red points is 2.6 m/s.

Fig. 3: The green and black lines are the reference and measured trajectories, respectively. The shaded regions represent the funnels around the reference trajectory. The goal of this experiment is to move inside of the pipe between the blue and red points safely.